On an alternative approach to pressure loads problems in topology optimization

Matteo Bruggi, Carlo Cinquini
Department of Structural Mechanics, University of Pavia, Italy
E-mail: matteo.bruggi@unipv.it, carlo.cinquini@unipv.it

Keywords: topology optimization, pressure loads, global stress constraints.

SUMMARY. The paper focuses on an alternative formulation for the topology optimization of structures acted upon by pressure loads according to the approach introduced in [1] and [2]. The method resorts to the modeling of an additional fluid phase within the topology optimization framework. The implementation of the incompressible phase enables to transfer pressure loads from the domain boundaries to the evolving edges of optimal design. The core of the approach herein presented consists in the adoption of a "truly–mixed" variational formulation [3] coupled to the enforcement of a global stress constraint that governs the pressure of the fluid phase. The proposed method is shown to achieve robust optimal designs for structures acted upon by pressure loads at a small computational effort. The adopted framework has peculiar advantages with respect to standard methods against the appearance of undesired cavities filled with fluid in final layouts.

1 INTRODUCTION

The paper proposes a formulation for the topology optimization of structures under pressure loads that is alternative to the classical frameworks presented in [4, 5].
Dealing with design–dependent loads, a crucial issue of the procedure consists in the achievement of an efficient procedure that transfers the loads originally assigned on the boundary of the domain to the edges of the evolving optimal design. Standard ways out to this trouble resort to the adoption of ad hoc algorithms that recover the load application surfaces at each step of the minimization process. To avoid the implementation of such kind of complex procedures [1] firstly proposed to introduce an additional fluid phase that enables the expected enforcement of the pressure loads on the evolving boundaries of the optimal design. The procedure mainly consists in the formulation of a multi–phase topology optimization setting for the achievement of the overall minimum compliance, thus taking into account a solid, a void and a liquid phase. The incompressible phase is assumed to have a bulk modulus $K \approx \infty$, with the aim of introducing a negligible bias in the evaluation of the overall compliance $\mathcal{C}$. According to the scheme above introduced the fluid phase allows for a straightforward implementation of standard topology optimization techniques that only require the adoption of robust finite element discretizations to cope with the incompressible phase. [1] overcame the problem adopting low order u-p formulations that were shown to achieve feasible solutions without the appearance of undesired oscillations at least in the examples considered in the work. A more affordable choice consists in the adoption of finite element discretizations that are fully stable with respect to the inf–sup condition of [3]. To this purpose one may resort to higher order u–p formulations [6] or move to the adoption of "truly–mixed" schemes. According to [2] the variational principle of Hellinger–Reissner [3] is herein considered and coupled to a discretization based on the composite element of Johnson and Mercier [7].
The above numerical framework allows to solve several problems of topology optimization for pressure loads but is not able to avoid the appearance of cavities filled with fluid. A classical way to

solve this trouble consists in the introduction of an additional volume constraint that controls the fluid volume fraction. An iterative procedure may be therefore set up to completely remove the filled cavities by progressively reducing the allowed fluid amount. This procedure considerably increases the computational burden since the optimization algorithm must be called several times and the optimal volume fraction that completely removes the filled cavities can not be achieved in a straightforward way.
Alternatively, the original formulation may be updated introducing suitable pressure enforcements, that allow to solve the problem in a single iteration, see [2]. This set of constraints introduces an upper bound to the pressure p of the fluid region, i.e. it enforces $p \leq \overline{p}$, where $\overline{p}$ is the external load. Focusing on the optimal designs that present holes filled with fluids it may be observed that these non–empty cavities experience higher pressures with respect to the fluid zones directly connected to the boundaries and therefore acted upon by the pressure $\overline{p}$. Prescribing an upper limit equal to $\overline{p}$ in every zone made of liquid phase, one may therefore expect to remove these undesired cavities. This approach may reduce the computing time with respect to the iterative procedure based on the evolving volume constraints. However, the adoption of many local enforcements increases the time needed by the optimization algorithm when minimizing the multi–constrained objective function. It is well–known in fact that many gradient–based algorithms, as the herein adopted Method of Moving Asymptotes (MMA)[8], decrease their performances with an increased number of local constraints.
Within the above framework the main aim of the present contribution is the improvement of the numerical efficiency of the topology optimization setting outlined above, i.e. the multi–phase formulation based on the control of the fluid pressure, as originally presented in [2]. The proposed approach takes full advantage of the features of the JM element, not only for its inherent stability in handling the incompressible phase but also for the accuracy in stress constraints imposition. The investigations presented in [9] suggest that the adoption of a global stress constraint may be a feasible choice if a nearly homogeneous stress state is expected in final designs. This is the case of the pressure field to be controlled.
A global stress constraint based on the η–mean of the fluid pressure is therefore herein implemented on the average degrees of freedom of the considered element. This is shown to produce the expected designs that are free from cavities filled by fluid, while a reduction of computational times may be also achieved.
The sequel of the paper introduces fundamentals of the adopted truly–mixed scheme along with the implemented multi–phase formulation for the minimum compliance design. Peculiar attention is paid to the global constraint on the fluid pressure along with the derivation of its sensitivities. Numerical simulations are shown to assess the capabilities of the method and to discuss its peculiar features on a benchmark example.

2 THE TRULY–MIXED APPROACH

A few theoretical remarks on the truly–mixed approach are herein recalled, pointing out peculiar issues on both the continuous and the discrete form as they will be exploited in the sequel. More details on the subject may be found in [3] and [7].

2.1 *The continuous formulation*

Let $\Omega \in R^2$ be a regular domain bounded by $\partial\Omega$ and $\underline{\underline{\underline{\underline{C}}}}$ the elasticity tensor of the linear elastic isotropic medium. $\underline{\underline{\sigma}}$ and $\underline{u}$ are the unknown stress and displacement fields, respectively, while $\underline{g}$ is the vector body load. $\underline{u}_d$ denotes the prescribed displacement on Γ_d, while $\underline{f}_t$ the prescribed traction on Γ_t, being, $\Gamma = \Gamma_d \cup \Gamma_t$. The truly–mixed variational principle consists of two groups of equations.

The first one couples constitutive law and compatibility, that are both tested by a virtual stress field $\underline{\underline{\tau}}$. The second one is the equilibrium, that is tested by means of the virtual displacement field $\underline{v}$. The "truly–mixed" weak formulation reads: find $(\underline{\underline{\sigma}}, \underline{u}) \in H \times W$ such that $\underline{\underline{\sigma}} \cdot \underline{n} \mid_{\Gamma_t} = \underline{f}_t$ and

$$\begin{cases} \displaystyle\int_\Omega \underline{\underline{\underline{\underline{C}}}}^{-1} \underline{\underline{\sigma}} : \underline{\underline{\tau}} dx + \int_\Omega \underline{\mathrm{div}}\, \underline{\underline{\tau}} \cdot \underline{u} dx = \int_{\Gamma_d} \underline{u}_d \cdot (\underline{\underline{\tau}} \cdot \underline{n}) ds, & \forall \underline{\underline{\tau}} \in H, \\ \displaystyle\int_\Omega \underline{\mathrm{div}}\, \underline{\underline{\sigma}} \cdot \underline{v} dx = -\int_\Omega \underline{g} \cdot \underline{v} dx, & \forall \underline{v} \in W. \end{cases} \tag{1}$$

where $\underline{n}$ denotes the normal vector to the boundary. It must be remarked that stresses are main variable of the problem and belong to a functional space that has strong regularity requirements, while displacements play the role of Lagrangian multipliers. This issue remarkably affects the discretization of the statement in Eqn. (1), that will be addressed in the next paragraphs.

2.2 *Finite element discretization*

The above variational principle is discretized within a bidimensional context resorting to the composite element of Johnson and Mercier [7], that passes the inf–sup requirement [3] for any compressibility condition of the involved material. This means that the finite element choice is fully stable even in the presence of the incompressible phase and no fluctuation or numerical instability is expected in the achieved numerical results. Each JM element K is made of three sub-triangles T_j. The displacement field is discretized via linear functions on the whole element, as done in classical displacement–based interpolation. The stress field is linearly interpolated within each sub–triangle and the continuity of the traction between each sub-edge is a priori imposed. Denoting with $P_1(T_j)$ the space of the polynomials of degree ≤ 1 on T_j, the space of approximation of stresses therefore reads:

$$H_h = \{\, \underline{\underline{\sigma}}_h \in H(\underline{\mathrm{div}}\,; \Omega),\ \underline{\underline{\sigma}}_h \in H(\underline{\mathrm{div}}\,; K),\ \underline{\underline{\sigma}}_h|_{T_j} \in [P_1(T_j)]^{2\times 2}_s,\ j = 1,2,3\}, \tag{2}$$

where $\underline{\underline{\sigma}}_h$ may be derived according to the following 15 degrees of freedoms:

$$\int_{e_i} (\underline{\underline{\sigma}}_h \cdot \underline{n}) \cdot \underline{w} ds, \quad \forall \underline{w} \in (P_1(e_i))^2, \quad i = 1,2,3, \tag{3}$$

$$\int_K \underline{\underline{\sigma}}_h : \underline{\underline{w}} dx, \quad \forall \underline{\underline{w}} \in (P_0(K))^{2\times 2}_s, \tag{4}$$

where e_i is the i–th edge of the triangular element K. Among the above degrees of freedom, the three unknowns introduced in Eqn. (4) are defined as the average of the components of the stress tensor on the whole triangle. This provides an accurate measure of the element–wise pressure p_i, that may be directly recovered performing the following computation on each triangle:

$$p_i = \frac{\sigma_{xx} + \sigma_{yy}}{2}. \tag{5}$$

The element–wise average pressure p_i is in fact derived taking into account only σ_{xx} and σ_{yy}, that are two of the three dofs defined in Eqn. (4). It must be remarked that the adoption of a JM–based discretization allows for a robust evaluation of both the displacement field and the stress one. Similar features may be achieved via u-p formulations only adopting higher order approximations with respect to those already considered in [1].

3 THE MULTI–PHASE TOPOLOGY OPTIMIZATION SETTING

As outlined in Section 1, the proposed approach is based on the adoption of a multi–phase topology optimization that minimizes the compliance of the overall structure with a volume constraint on the amount of material for the optimal design. To control the arising of cavities filled with fluid, the adoption of a global stress constraint on the fluid pressure is also included in the formulation.

3.1 *The "bi–material with void" interpolation*

The stiffness penalization resorts to the adoption of two design variables, i.e. ρ_0 and ρ. The first interpolates between the cases where there is material or not, according to a classic SIMP (Solid Isotropic Material with Penalization). The second one adopts a RAMP (Rational Approximation of Material Properties) to model the variation between the fluid and the solid phase. Reference is made to [10] for a detailed review on the above material models. The adopted "bi–material with void" scheme reads as follows:

$$\begin{aligned} K(\rho,\rho_0) &= \rho_0^s \ (K_m + \frac{1-\rho}{1+q(\rho)}(K_f - K_m)), \\ G(\rho,\rho_0) &= \rho_0^t \ (G_f + \frac{\rho}{1+r(1-\rho)}(G_m - G_f)), \end{aligned} \tag{6}$$

where K_m and G_m are respectively the bulk and shear modulus of the elastic compressible material, while K_f and G_f refer to the fluid phase. Peculiar attention must be paid in order to avoid the arising of undesired numerical instabilities related to the presence of an incompressible phase [1, 11]. To this purpose the simulations presented in the sequel follow the assumptions $q = r = 3$ and $s = 6 > t = 3$, as discussed in [2]. Referring to the fluid component, the relevant values of the material properties adopted in the simulations are $K_f = 200K_m$ and $G_f = 10^{-6}$.

3.2 *The pressure–constrained optimal problem*

The following discrete scheme for the topology optimization of structures that are acted upon by pressure loads is implemented:

$$\begin{cases} \min\limits_{\rho,\rho_0} \quad \mathcal{C} & = \ \overline{P}^t U \\ \text{s.t.} \quad \begin{bmatrix} A_{\sigma\sigma}(\rho,\rho_0) & B_{\sigma u} \\ B_{u\sigma} & 0 \end{bmatrix} \begin{Bmatrix} \sigma \\ u \end{Bmatrix} & = \ \begin{Bmatrix} f \\ g \end{Bmatrix} \\ \sum\limits_{i=1}^{N} \rho_i \rho_{0i} A_i & \leq \ \overline{V} \\ \left[\frac{1}{N} \sum\limits_{i=1}^{N} (1-\rho_i) \left(\frac{p_i}{\overline{p}} \right)^{\eta} \right]^{1/\eta} & \leq 1 \\ 0 < \rho_i \leq 1 & \\ 0 < \rho_{0i} \leq 1. & \end{cases} \tag{7}$$

In the above equation $\overline{P}$ is the external load vector that enforces the pressure $\overline{p}$, $U \subset u$ the dual displacements, while ρ and ρ_0 are two vectors of unknowns for the design interpolation introduced

in Section 3.1. According to an element–wise discretization of the density variables, two unknowns ρ_i and ρ_{0i} are assigned to each one of the N triangles in the mesh.
The constraint in Eqn. $(7)_1$ enforces the discrete truly–mixed form of the elasticity problem descending from the continuous statement of Eqn. (1). It also points out the the overall compliance matrix only depends on the density unknowns through the bilinear form $A_{\sigma\sigma}$.
Eqn. $(7)_2$ simply represents the volume constraint, enforcing $\overline{V}$ as the maximum admissible volume of solid material, i.e. an assigned fraction of the total design domain volume V_{tot}. A_i is in fact the bidimensional dimension of the i–th element.
Eqn. $(7)_3$ is the global pressure constraint that is formulated through an η–mean measure on the N element–wise pressure p_i, see [12]. The dependence on ρ_i is introduced with the aim of reducing the constraint imposition to the fluid region. The solid phase, i.e. $\rho = 1$, does not provide in fact any contribution to the sum in Eqn. $(7)_3$, whatever the amount of material ρ_0. In order to avoid the presence of negative terms, the adopted values of η must be chosen within the even numbers. Focusing on the asymptotic behavior of the η–mean global measure, it must be remarked that the maximum pressure $\overline{p}$ is always bounded from below by the herein considered constraint. The values of η that are generally adopted in the simulations ($\eta = 4$ in the investigations further presented) are especially conceived to improve the numerical tractability of the problem within the optimization algorithm, but may weaken the effectiveness of the enforcement. A suitable decrease of $\overline{p}$ with respect to the value of the external pressure may be therefore considered in order to lessen the above bias in the numerical implementation of Eqn. $(7)_3$.

3.3 *Computational details*

The problem in Eqn. (7) is solved through the adoption of the Method of Moving Asymptotes (MMA) [8] in conjunction with the analytical computations of the gradients. A crucial issue of the proposed procedure hence resides in the handling of the sensitivities of the global stress constraint. The derivative of Eqn. $(7)_3$, called c, with respect to a generic density unknown, called ρ_k (of the type ρ_i or ρ_{0i}), may be straightforwardly written as:

$$\frac{\partial c}{\partial \rho_k} = \frac{1}{\eta}\left[\frac{1}{N}\sum_{i=1}^{N}(1-\rho_i)\left(\frac{p_i}{\overline{p}}\right)^{\eta}\right]^{1/\eta-1} \cdot \frac{1}{N}\sum_{i=1}^{N}\left[-\delta_{ik}\left(\frac{p_i}{\overline{p}}\right)^{\eta} + (1-\rho_i)\left(\frac{p_i}{\overline{p}}\right)^{\eta-1}\frac{\eta}{\overline{p}}\frac{\partial p_i}{\partial \rho_k}\right], \tag{8}$$

where δ_{ik} is the Kronecher delta, i.e. $\delta_{ik} = 1$ for $\rho_i = \rho_k$, otherwise $\delta_{ik} = 0$. One has to take into account that the derivatives of the element–wise average pressure p_i with respect to the density unknowns may be directly solved via a simple analytical computation. This descends from the adoption of the criterion in Eqn. (5) and the independent stress interpolation within the truly–mixed variational principle. One may derive the sensitivities of the relevant average degrees of freedom, of the type in Eqn. (4), from a set of auxiliary mixed problems:

$$\begin{bmatrix} A_{\sigma\sigma}(\rho,\rho_0) & B_{\sigma u} \\ B_{u\sigma} & 0 \end{bmatrix} \begin{Bmatrix} \dfrac{\partial \sigma}{\partial \rho_k} \\ \\ \dfrac{\partial u}{\partial \rho_k} \end{Bmatrix} = - \begin{bmatrix} \dfrac{\partial A_{\sigma\sigma}}{\partial \rho_k} & 0 \\ \\ 0 & 0 \end{bmatrix} \begin{Bmatrix} \sigma \\ u \end{Bmatrix}. \tag{9}$$

Referring to the finite element interpolation, it must be finally remarked that the saddle–point nature of the mixed problem leads to a solving matrix in Eqn. $(7)_1$ that is not positive defined. To this purpose peculiar solvers must be adopted as reported in [13].

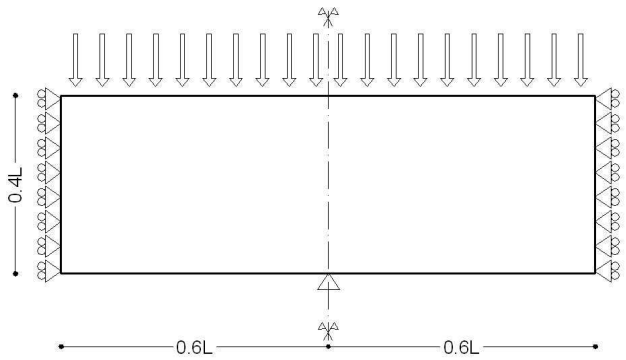

Figure 1: The piston problem.

To assess the capabilities of the proposed algorithm, the problem depicted in Figure 1 is considered. The benchmark consists in finding the optimal design of a piston whose upper edge is acted upon by a pressure load $\overline{p} = 1$, allowing for $\overline{V} = 0.3V_{tot}$.
The original domain is firstly optimized under fixed loads, i.e. adopting a standard formulation for volume–constrained minimum compliance that resorts to a classical mono–material interpolation. The result is shown in Figure 2, achieving a final compliance $\mathcal{C} = 8.061$. Black regions mean solid material, while white domains define the void zones.
The numerical scheme presented in Section 3.2 is subsequently implemented without taking into account the global pressure constraint of Eqn. $(7)_3$. The achieved result is shown in Figure 3 ($\mathcal{C} = 6.742$), where grey regions define the additional fluid phase. The figure also presents the relevant pressure map of the optimal layout.
As outlined in Section 1, the fluid in the filled cavity is more stressed with respect to the external pressure $\overline{p}$. This suggests the idea that suitable pressure constraints may be able of controlling the arising of filled cavities. The achievement of different enclosed zones with equal pressure has no peculiar advantage on the optimal designs. The same result may be achieved via a direct connection of the filled zones, thus reducing the amount of solid material that separates the cavities.
According to the above discussion the whole Eqn. (7) is therefore implemented, taking into account the η–mean constraint on the fluid pressure. Figure 4 shows the achieved optimal design

Figure 2: Optimal design for fixed load.

($\mathcal{C} = 7.501$), that is in full agreement with the layout obtained via the adoption of local pressure constraints in [2] and is also very similar to the result based on iterative volume enforcements on the fluid fraction in [1].
It must be remarked that the proposed approach allows to reduce the computational time needed to solve the problem with respect to the alternative methods above mentioned. A single optimization based on two constraints may be much more efficient with respect to multi–constrained formulations or iterative approaches. However one has to take into account that the asymptotic nature of the η–mean and the values of η that are usually assumed in the simulations may require a suitable setting of the value $\overline{p}$ to be implemented in Eqn. $(7)_3$.

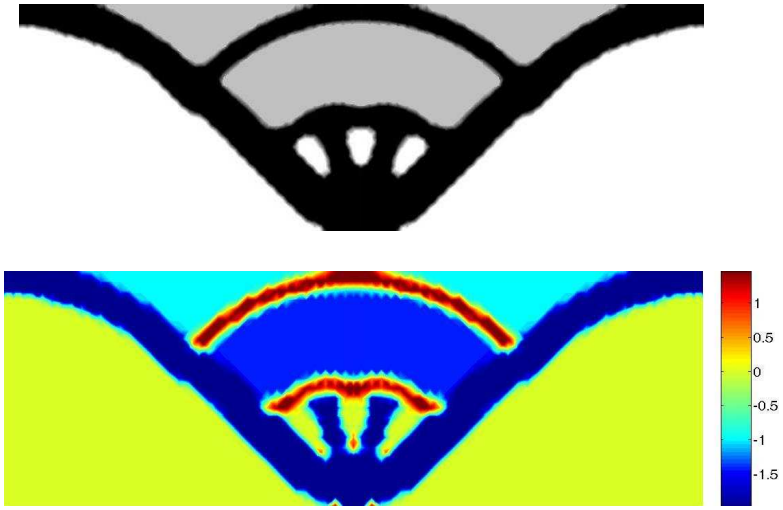

Figure 3: Optimal design for pressure load (without the global constraint in Eqn. $(7)_3$) and relevant pressure map.

Figure 4: Optimal design for pressure load with the global constraint in Eqn. $(7)_3$.

5 CONCLUSIONS

The paper has dealt with an alternative formulation to cope with the topology optimization of structures that are acted upon by pressure loads. The method is based on the modeling of an additional fluid phase that allows to transfer the pressure forces from the boundaries of the original

domain to the evolving edges of the optimal design. A minimum compliance volume–constrained formulation has been therefore implemented resorting to the adoption of a "truly–mixed" variational formulation coupled to the enforcement of a global stress constraint that governs the pressure of the fluid phase. The truly–mixed scheme provides the required robustness in the evaluation of both the displacement and the stress field, while the global constraint exhibits peculiar advantages against the achievement of undesired cavities filled with fluid in final layouts. Due to the homogeneity of the pressure field to be controlled, the adoption of a single global enforcement may be considered a feasible alternative to more demanding multi–constrained formulations. Further investigations are needed to investigate the sensitivity of the proposed algorithm with respect to the parameters involved in the imposition of the global pressure constraint.

References

[1] Sigmund O. and Clausen P.M. Topology optimization using a mixed formulation: An alternative way to solve pressure load problems *Comput. Methods Appl. Mech. Eng.* 2007; **196**: 1874–1889.

[2] Bruggi M. and Cinquini C. An alternative truly–mixed formulation to solve pressure load problems in topology optimization *Comput. Methods Appl. Mech. Eng.* 2009; **198**: 1500–1512.

[3] Brezzi F. and Fortin M., 1991. Mixed and Hybrid Finite Element Methods. Springer–Verlag, New York.

[4] Chen B.–C. and Kikuchi N. Topology optimization with design dependent loads. *Finite Element in Analysis and Design* 2001; **37**:57–70.

[5] Hammer V.B. and Olhoff N. Topology optimization of continuum structures subjected to pressure loading.*Struct. Multidisc. Optim.* 2000; **19**:85–92.

[6] Braess D., 1997. Finite Elements. Cambridge University Press.

[7] Johnson. C. and Mercier B. Some equilibrium finite elements methods for two dimensional elasticity problems. *Numer. Math.* 1978; 30, 103–116.

[8] Svamberg K. Method of moving asymptotes - A new method for structural optimization. *International Journal for Numerical Methods in Engineering* 1987; **24**(3):359–373.

[9] Bruggi M. and Duysinx P. On the use of a truly-mixed formulation in topology optimization with global stress-constraints *Eighth World Congress on Structural and Multidisciplinary Optimization*, 2009.

[10] Bendsøe M. P. and Sigmund O., 2003. Topology optimization - Theory, methods and applications, Springer, EUA, New York.

[11] Bruggi M. and Venini P. Topology optimization of incompressible media using mixed finite elements *Comput. Methods Appl. Mech. Eng.* 2007; **196**:3151-3164.

[12] Duysinx P. and Sigmund O. New developments in handling stress constraints in optimal material distribution. *Seventh Symposium on Multidisciplinary Analysis and Optimization*, AIAA-98-4906, 1501-1509, 1998.

[13] Schenk O. and Gärtner K. Solving Unsymmetric Sparse Systems of Linear Equations with PARDISO, *Journal of Future Generation Computer Systems* 2004; **20(3)**:475–487.